

ASTROMETRIC MICROLENSING OF STARS

MARTIN DOMINIK^{1,2} AND KAILASH C. SAHU¹*e-mail:* dominik@astro.rug.nl, ksahu@stsci.edu

ABSTRACT

Due to dramatic improvements in the precision of astrometric measurements, the observation of light centroid shifts in observed stars due to intervening massive compact objects (‘astrometric microlensing’) will become possible in the near future. Upcoming space missions, such as SIM and GAIA, will provide measurements with an accuracy of 4–60 μas depending on the magnitude of the observed stars, and an accuracy of $\sim 1 \mu\text{as}$ is expected to be achieved in the more distant future. There are two different ways in which astrometric microlensing signals can be used to infer information: one possibility is to perform astrometric follow-up observations on photometrically detected microlensing events, and the other is to perform a survey based on astrometric observations alone. After the predictable effects of the Sun and the planets, stars in the Galactic disk play the dominant role in astrometric microlensing. The probability that the disk stars introduce a centroid shift larger than the threshold δ_T at a given time for a given source in the Galactic bulge towards Baade’s window reaches 100% for a threshold of $\delta_T = 0.7 \mu\text{as}$, while this probability is $\sim 2\%$ for $\delta_T = 5 \mu\text{as}$. However, this centroid shift does not vary much during the time in which a typical photometric microlensing event differs from baseline. So astrometric follow-ups (e.g. with SIM) are not expected to be disturbed by the statistical astrometric microlensing due to disk stars, so that it is possible to infer additional information about the nature of the lens that caused the photometric event, as suggested. The probability to observe astrometric microlensing events within the Galaxy turns out to be large compared to photometric microlensing events. The probability to see a variation by more than $5 \mu\text{as}$ within one year and to reach the closest angular approach between lens and source is $\sim 10^{-4}$ for a bulge star towards Baade’s window, while this reduces to $\sim 6 \cdot 10^{-6}$ for a direction perpendicular to the Galactic plane. For the upcoming mission GAIA, we expect ~ 1000 of the observed stars to show a detectable astrometric microlensing signal within its 5 year lifetime. These events can be used to determine accurate masses of the lenses, and to derive the mass and the scale parameters (length and height) of the Galactic disk.

Subject headings: astrometry – galaxy: structure – galaxy: stellar content – gravitational lensing

1. INTRODUCTION

It is known for more than one decade (Paczynski 1986) that the nature of matter between the observer and observed source stars can be studied by observing brightenings of a large number of these stars caused by the deflection of light by the intervening material. In addition to this magnification effect, there is also a shift in the light centroid of the observed star introduced by the lens object (Høg, Novikov, & Polnarev 1995; Miyamoto & Yoshii 1995; Walker 1995). Upcoming space missions will enable us to observe this centroid shift (Paczynski 1998; Boden, Shao, & Van Buren 1998). In particular, the Space Interferometry Mission (SIM, Allen et al. 1997)³ will allow observations of selected targets with a positional accuracy of $\sim 4 \mu\text{as}$ for sources brighter than $V = 20$. Moreover, the Global Astrometric Interferometer for Astrophysics mission (GAIA, Lindegren & Perryman 1996)⁴ will perform an astrometric survey aimed at all-sky coverage (Gilmore et al. 1998) with an accuracy of $20 \mu\text{as}$ ($60 \mu\text{as}$) for sources with $V < 12$ ($V < 15$).⁵ These two missions are somewhat complementary: While SIM has the ability to point the instrument to selected targets, it will not perform a large survey program; on the other hand, GAIA will perform an all-sky survey, but will not have the ability to point

the instrument to a selected target.

It has been mentioned (Paczynski 1998; Boden et al. 1998; Høg et al. 1995; Miyamoto & Yoshii 1995; Walker 1995) that the observation of the centroid shift during a (photometrically discovered) microlensing event will yield additional information about the lens, so that its mass, distance, and velocity can be determined unambiguously.

Most of the discussions in the literature so far have been confined to the centroid shifts of photometrically detected microlensing events which can be detected by an instrument like SIM (e.g. Paczynski 1998; Boden et al. 1998). It has been pointed out, however, that the microlensing cross-section for centroid shift measurements is much larger than the cross-section for light amplification (Paczynski 1996; Miralda-Escudé 1996). In this paper, we investigate the effects of disk stars on the astrometric microlensing signal (centroid shift). The disk stars can affect this signal in two ways. First, for a microlensing event that has been detected by its photometric signal, the intervening matter can lead to additional centroid shifts and variations of these shifts with time, which disturb the signal of the centroid shift caused by the lens responsible for the photometrically detected microlensing event. Second, the disk

¹Space Telescope Science Institute, 3700 San Martin Drive, Baltimore, MD 21218, USA

²Kapteyn Astronomical Institute, Postbus 800, 9700 AV Groningen, The Netherlands

³for information about SIM see also <http://sim.jpl.nasa.gov>

⁴for information about GAIA see also <http://astro.estec.esa.nl/SA-general/Projects/GAIA/gaia.html>

⁵Throughout the paper, we are talking about the accuracy of single astrometric measurements, not the accuracy of parallax measurements obtained from the mission within its lifetime.

stars form a population producing microlensing events that can be detected by their astrometric microlensing signal alone in an astrometric survey such as GAIA.

This paper is organized as follows. We discuss the signals of photometric and astrometric microlensing in Sect. 2. In Sect. 3, the optical depths due to photometric and astrometric microlensing and the differences are discussed. The characteristics of astrometric microlensing events and the prospects for disk stars as lenses are discussed in Sect. 4. In Sect. 5, we show that by observing astrometric microlensing events towards several directions, one can measure the scale parameters of the mass distribution of the Galactic disk. In Sect. 6, the effect of a luminous lens is discussed, while the implications for upcoming space missions are discussed in Sect. 7. Finally, in Sect. 8, the results of the previous sections are summarized.

2. THE SIGNALS OF PHOTOMETRIC AND ASTROMETRIC MICROLENSING

Though the magnification of the source and the shift of its centroid of light are based on the same effect, there are some qualitative differences in the observable signals.

Let the source be located at a distance D_S from the observer and the lens with mass M at a distance $0 < D_L < D_S$ from the observer. Let $\vec{\varphi}_L$ and $\vec{\varphi}_S$ denote the angular positions of the lens and source respectively. One can then define a dimensionless distance vector

$$\vec{u} = \frac{\vec{\varphi}}{\theta_E} = \frac{\vec{\varphi}_S - \vec{\varphi}_L}{\theta_E}, \quad (1)$$

where

$$\theta_E = \sqrt{\frac{4GM}{c^2} \frac{D_S - D_L}{D_S D_L}} \quad (2)$$

is the angular Einstein radius. The Einstein radius

$$r_E = D_L \theta_E = \sqrt{\frac{4GM}{c^2} \frac{D_L (D_S - D_L)}{D_S}} \quad (3)$$

gives the physical size of the angular Einstein radius in a plane perpendicular to the line-of-sight observer-source at the position of the lens (lens plane).

In the following, we assume that there is no light contribution from an unresolved luminous lens. The validity of this approximation and possible modifications due to a luminous lens are discussed in Sect. 6.

The magnification of the source due to the lens is given by (e.g. Paczyński 1986)

$$\mu(u) = \frac{u^2 + 2}{u\sqrt{u^2 + 4}}, \quad (4)$$

where $u = |\vec{u}|$.

For $u \ll 1$, one has

$$\mu(u) \simeq \frac{1}{u}, \quad (5)$$

and for $u \gg 1$, one has

$$\mu(u) \simeq 1 + \frac{2}{u^4}, \quad (6)$$

so that for large angular separations, the lensed star produces a magnitude shift of

$$\Delta \text{mag} = -\frac{5}{\ln 10} \frac{1}{u^4}. \quad (7)$$

The centroid shift of the source for a dark lens given by (Høg et al. 1995; Miyamoto & Yoshii 1995; Walker 1995)

$$\vec{\delta}(\vec{u}) = \frac{\vec{u}}{u^2 + 2} \theta_E, \quad (8)$$

i.e. it points away from the lens as seen from the source.

For $u \gg \sqrt{2}$, one has

$$\delta(u) \simeq \frac{1}{u} \theta_E, \quad (9)$$

so that the centroid shift falls off much more slowly than the magnitude shift towards larger u . For $u \ll \sqrt{2}$,

$$\delta(u) \simeq \frac{u}{2} \theta_E, \quad (10)$$

i.e. for small separations, the centroid shift tends linearly to zero, while the magnification increases towards smaller separations. In contrast to the magnification, the absolute centroid shift reaches a maximum at $u = \sqrt{2}$ which is

$$\delta_{\text{max}} = \frac{\sqrt{2}}{4} \theta_E \approx 0.354 \theta_E. \quad (11)$$

While the magnification is a dimensionless scalar, the centroid shift is a vector with dimension, and therefore it depends not only on the dimensionless separation u , but is also proportional to the characteristic angular scale θ_E .

If one neglects the parallactic motion, the relative path between lens and source is a straight line, so that

$$u(t) = \sqrt{u_0^2 + [p(t)]^2}, \quad (12)$$

where

$$p(t) = \frac{t - t_0}{t_E}. \quad (13)$$

This means that the closest approach between lens and source occurs at time t_0 , where $|\vec{u}| = u_0$, and

$$t_E = \frac{\theta_E}{\mu}, \quad (14)$$

where μ is the relative proper motion between source and lens.

The absolute value of the centroid shift then reads

$$\delta(u_0, p) = \frac{\sqrt{u_0^2 + p^2}}{u_0^2 + p^2 + 2} \theta_E, \quad (15)$$

and the components against the direction of the motion of the lens relative to the source δ_{\parallel} (i.e. in the direction of the motion of the source relative to the lens) and perpendicular to it towards the side where the source is passed as seen by a moving lens (i.e. away from the lens as seen by a moving source) δ_{\perp} are

$$\begin{aligned} \delta_{\parallel}(u_0, p) &= \frac{p}{u_0^2 + p^2 + 2} \theta_E, \\ \delta_{\perp}(u_0, p) &= \frac{u_0}{u_0^2 + p^2 + 2} \theta_E. \end{aligned} \quad (16)$$

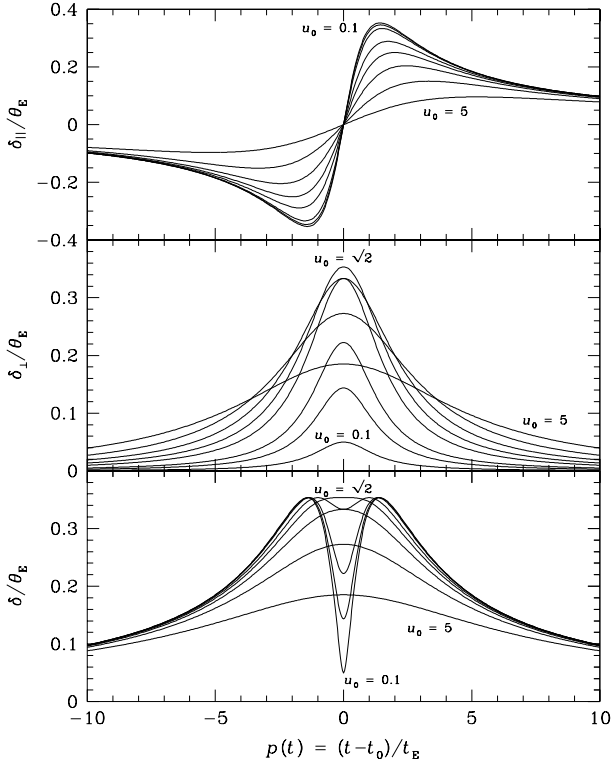


FIG. 1.— The absolute centroid shift δ and its components along the direction of motion (δ_{\parallel}) and perpendicular to it (δ_{\perp}) as a function of p for the minimum separations $u_0 = 0.1, 0.3, 0.5, 1.0, \sqrt{2}, 2.0, 3.0,$ and 5.0 . *Top panel:* The parallel component δ_{\parallel} . The curves are antisymmetric with respect to $p = 0$, the steepest curve corresponds to $u_0 = 0.1$ and the flattest curve to $u_0 = 5$. *Middle panel:* The perpendicular component δ_{\perp} . The curves are symmetric with respect to $p = 0$. At $p = 0$, the largest value, namely $\sqrt{2}/4$, is reached for $u_0 = \sqrt{2}$; $u_0 = 1$ and $u_0 = 2$ yield the same $\delta_{\perp}(u_0, 0)$. For large given $|p|$, $\delta_{\perp}(u_0, p)$ decreases with smaller u_0 . *Bottom panel:* The absolute value of the centroid shift δ . The curves are symmetric with respect to $p = 0$. The largest value at $p = 0$ is reached for $u_0 = \sqrt{2}$, namely $\sqrt{2}/4$. For $u_0 \geq \sqrt{2}$, there is a maximum at $p = 0$, while for $u_0 < \sqrt{2}$ a minimum occurs. $u_0 = 1$ and $u_0 = 2$ yield the same $\delta(u_0, 0)$.

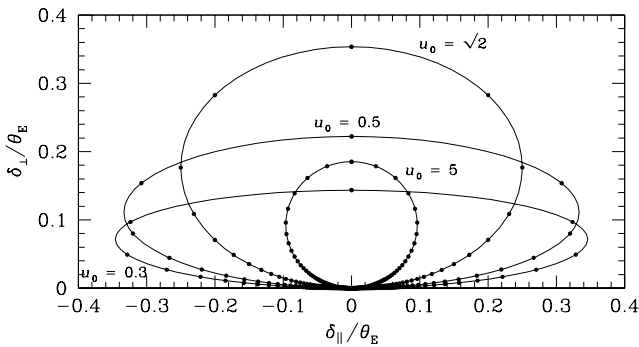


FIG. 2.— The centroid shift trajectory in $(\delta_{\parallel}, \delta_{\perp})$ -space for selected values of u_0 (where the brightness of the lens is neglected, see text for details). The centroid shift traces out an ellipse. The small dots on the trajectory mark points of time spaced by t_E .

These functions are shown in Fig. 1 for several values of u_0 . While δ_\perp is symmetric around $p = 0$ and always positive, δ_\parallel is antisymmetric. δ_\parallel has a maximum at $p = p_{m,\perp}$ and a minimum at $p = -p_{m,\perp}$, where

$$p_{m,\perp} = \sqrt{u_0^2 + 2} \quad (17)$$

and

$$\delta_\parallel(u_0, p_{m,\perp}) = \frac{1}{2\sqrt{u_0^2 + 2}} \theta_E. \quad (18)$$

For $u_0 \ll 1$, one obtains

$$p_{m,\perp} \simeq \sqrt{2} \quad (19)$$

and

$$\delta_\parallel(u_0, p_{m,\perp}) \simeq \delta_{\max}. \quad (20)$$

δ_\perp reaches a maximum at $p = 0$, where the height of the peak is maximal for $u_0 = \sqrt{2}$, reaching $\delta_\perp = \delta_{\max}$, and in general the peak height is

$$\delta_\perp(u_0, 0) = \frac{u_0}{u_0^2 + 2} \theta_E. \quad (21)$$

Since the absolute centroid shift has a maximum at $u = \sqrt{2}$, $\delta(u_0, p)$ goes through a minimum at $p = 0$ for $u_0 < \sqrt{2}$ and has two maxima at $p = \pm p_m$, where

$$p_m = \sqrt{2 - u_0^2}, \quad (22)$$

i.e. $u = \sqrt{u_0^2 + p^2} = \sqrt{2}$, so that $\delta(u_0, p_m) = \delta_{\max}$. Note that for $u_0 \ll 1$, $p_m \simeq \sqrt{2}$, so that $p_m \simeq p_{m,\perp}$. For $u_0 \geq \sqrt{2}$, δ has only one maximum at $p = 0$, where

$$\delta(u_0, 0) = \delta_\perp(u_0, 0) = \frac{u_0}{u_0^2 + 2} \theta_E. \quad (23)$$

Note that $\delta(u_1, 0) = \delta(u_2, 0)$ for $u_1 u_2 = 2$.

For large $|p|$, $\delta_\perp \propto 1/p^2$, while $\delta_\parallel \propto 1/p$, so that $\vec{\delta}$ points nearly against the direction of the motion of the lens relative to the source for large p and into it for small p , so that the direction of the motion can be identified easily: the change of the centroid shift is in the direction of the lens motion for large $|p|$. Due to the symmetry of δ_\perp and the antisymmetry of δ_\parallel , the vector

$$\vec{\delta}_\perp = \frac{1}{2} \left(\vec{\delta}(u_0, p) + \vec{\delta}(u_0, -p) \right) \quad (24)$$

points perpendicular to the lens motion relative to the source towards the side where the source is passed and the vector

$$\vec{\delta}_\parallel = \frac{1}{2} \left(\vec{\delta}(u_0, p) - \vec{\delta}(u_0, -p) \right) \quad (25)$$

points against the direction of the motion of the lens relative to the source for $p > 0$ and into it for $p < 0$.

In $(\delta_\parallel, \delta_\perp)$ -space, the centroid-shift trajectory is an ellipse (e.g. Walker 1995) with semi-major axis a in the δ_\parallel -direction and semi-minor axis b in the δ_\perp -direction centered at $(0, b)$, where

$$a = \frac{1}{2} \frac{1}{\sqrt{u_0^2 + 2}} \theta_E, \quad b = \frac{1}{2} \frac{u_0}{u_0^2 + 2} \theta_E. \quad (26)$$

For $u_0 \rightarrow \infty$, this ellipse becomes a circle with radius $\theta_E/(2u_0)$, and for $u_0 \rightarrow 0$, the ellipse degenerates into a straight line of length $\theta_E/\sqrt{2}$ (e.g. Walker 1995). For selected values of u_0 , the centroid-shift trajectory is shown in Fig. 2.

3. OPTICAL DEPTHS FOR PHOTOMETRIC AND ASTROMETRIC MICROLENSING

Let σ denote an area in the lens plane for which source positions projected onto the lens plane yield a certain microlensing signature. The probability γ to observe such a signature for a given source is then given by the product of the number area density of lenses and the area σ . With $\rho(x)$ being the mass volume density at the distance $D_L = x D_S$, and $f_M(M) dM$ being the distribution of lens masses, one obtains γ due to lenses at any distance between source and observer as

$$\gamma = D_S \int_0^1 \int_0^\infty \frac{\rho(x)}{M} \sigma(x, M) f_M(M) dM dx. \quad (27)$$

For photometric microlensing, a commonly used signature is the magnification of the light of the source star by more than a threshold μ_T at a given time, and the associated probability is referred to as optical depth of photometric microlensing τ_μ . This signature holds if the angular separation between the lens and the source is smaller than a corresponding threshold u_T , given by the inversion of Eq. (4) as

$$u_T = \sqrt{\frac{2}{\sqrt{1 - \mu_T^{-2}}}} - 2, \quad (28)$$

and $u_T = 1$ corresponds to $\mu_T = 3/\sqrt{5} \approx 1.34$. Therefore, $\sigma = \pi u_T^2 r_E^2$ in this case, and the optical depth reads

$$\tau_\mu(u_T) = u_T^2 \tau_\mu(1), \quad (29)$$

where

$$\tau_\mu(1) = \frac{4\pi G}{c^2} D_S^2 \int_0^1 \rho(x) x(1-x) dx. \quad (30)$$

Note that τ_μ does not depend on the masses of the lenses and that, in addition to distances with large ρ , objects around half-way between the observer and the source are favored.

Let us now consider a similar signature for the centroid shift, namely the case where the centroid shift exceeds a given threshold δ_T . From Eq. (8) one obtains that the absolute centroid shift exceeds a given threshold δ_T if $u \in [u_T^-, u_T^+]$, where

$$u_T^\pm = \frac{\theta_E}{2\delta_T} \pm \sqrt{\frac{\theta_E^2}{4\delta_T^2} - 2} \quad (31)$$

and $u_T^+ > \sqrt{2} > u_T^-$ for $\delta_T < \delta_{\max} = (\sqrt{2}/4) \theta_E$. Otherwise, there are no solutions due to the fact that δ_T cannot exceed δ_{\max} . Since the centroid shift is not a dimensionless quantity, u_T^\pm depend on θ_E , whereas for photometric signatures, u_T depends only on the magnification threshold μ_T and not on any other quantity. For $K = \theta_E/\delta_T \gg 1$

$$u_T^+ \simeq \frac{\theta_E}{\delta_T}, \quad u_T^- \simeq 2 \frac{\delta_T}{\theta_E}, \quad (32)$$

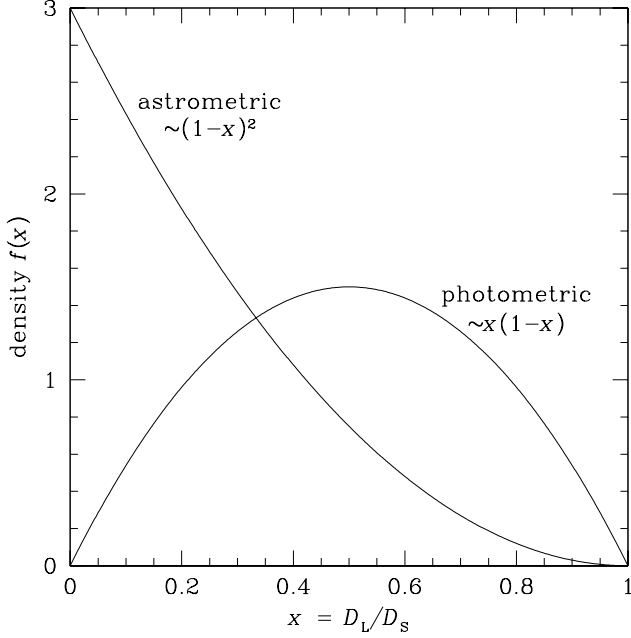


FIG. 3.— Density functions $f(x)$ for photometric microlensing ($f_1(x) = 6x(1-x)$) and astrometric microlensing ($f_2(x) = 3(1-x)^2$) showing the favored and disfavored values for the lens distance $D_L = x D_S$. The functions $f_i(x)$ are normalized, so that $\int_0^1 f_i(x) dx = 1$.

which also correspond to the large separation and small separation limits, Eqs. (9) and (10). As we will see in more detail in the next section, θ_E is of order mas, while δ_T is of order μ as, so that this is a fair approximation.

Since the area in the lens plane giving a centroid shift larger than δ_T is given by $\pi[(u_T^+)^2 - (u_T^-)^2] r_E^2$, and

$$(u_T^+)^2 - (u_T^-)^2 = K^2 \sqrt{1 - \frac{8}{K^2}} \simeq K^2 - 4 - \frac{8}{K^2}, \quad (33)$$

the optical depth for centroid shifts larger than δ_T can be written as

$$\tau_\delta(u_T^-, u_T^+) \simeq \tau_\delta(0, \theta_E/\delta_T) - 4\tau_\mu(1), \quad (34)$$

i.e. the corresponding area can be approximated by a circle with radius $u_T = \theta_E/\delta_T$, so that the upper threshold becomes $u_T^+ \simeq u_T$ and the lower threshold becomes $u_T^- \simeq 0$. This means that $\sigma = \pi u_T^2 r_E^2 = \pi D_L^2 \theta_E^4 / \delta_T^2$ and with Eq. (27), τ_δ reads

$$\begin{aligned} \tau_\delta(0, \theta_E/\delta_T) &= \pi D_S \int_0^1 \int_0^\infty \frac{\rho(x)}{M} \frac{D_L^2 \theta_E^4}{\delta_T^2} f_M(M) dM dx \\ &= \frac{16\pi G^2}{c^4} \frac{D_S \overline{M}}{\delta_T^2} \int_0^1 \rho(x) (1-x)^2 dx, \end{aligned} \quad (35)$$

where

$$\overline{M} = \int_0^\infty M f_M(M) dM \quad (36)$$

is the average mass from the mass spectrum f_M .

Contrary to photometric microlensing, small distances between observer and lens are favored, so that disk stars give the

main contribution. In addition, large distances between observer and lens are disfavored compared to photometric microlensing (see Fig. 3). While the bulge stars and the LMC stars may play an important role in the photometric microlensing towards the bulge (Kiraga & Paczyński 1994) and the LMC (Sahu 1994), respectively, their contribution to astrometric microlensing is very small.

From the expression for the optical depth τ_δ , Eq. (35), one sees that a probability density for a lens yielding a deflection above a given threshold at any time is given by

$$f_x(x) = C_0 \frac{d\tau_\delta}{dx} = C_1 \rho(x) (1-x)^2, \quad (37)$$

so that the expectation value for the lens distance is given by

$$\langle x \rangle = \frac{\int_0^1 \rho(x) x (1-x)^2 dx}{\int_0^1 \rho(x) (1-x)^2 dx}. \quad (38)$$

For constant mass density $\rho(x) = \rho_0$, one obtains

$$\langle x \rangle = \frac{\int_0^1 x (1-x)^2 dx}{\int_0^1 (1-x)^2 dx} = \frac{1}{4}. \quad (39)$$

After having established that the main contribution comes from close lenses, we can estimate the detection threshold for $D_S \gg D_L$: The angular Einstein radius θ_E reads in this limit

$$\begin{aligned} \theta_E &= \sqrt{\frac{4GM}{c^2 D_L}} \\ &= 2.0 \left(\frac{M}{0.5 M_\odot} \right)^{1/2} \left(\frac{D_L}{1 \text{ kpc}} \right)^{-1/2} \text{ mas}, \end{aligned} \quad (40)$$

For the maximum separation u_T yielding a signal above the

threshold δ_T , one obtains

$$u_T \simeq 2000 \left(\frac{M}{0.5 M_\odot} \right)^{1/2} \left(\frac{D_L}{1 \text{ kpc}} \right)^{-1/2} \left(\frac{\delta_T}{1 \mu\text{as}} \right)^{-1}. \quad (41)$$

Note that this is a gigantic number compared to photometric microlensing which yields a magnification 1% above the baseline for $u = 3.8$, while for $u = 200$, the magnification is only by a factor $1.4 \cdot 10^{-9}$ above the baseline, and for $u = 2000$, this reduces to $1.4 \cdot 10^{-13}$.

Let us also look how the centroid shift varies with time, i.e. consider a variation in the angular separation between lens and source described by a proper motion $\mu = d\varphi/dt = v/D_L$. Assuming the lens to be dark or resolved from the source, the change in the centroid shift is given by

$$\frac{d\delta}{du} = \frac{2 - u^2}{(u^2 + 2)^2} \theta_E, \quad (42)$$

which gives for $u \gg 1$

$$\frac{d\delta}{du} \simeq -\frac{1}{u^2} \theta_E, \quad (43)$$

or expressed with $\varphi = u \theta_E$

$$\frac{d\delta}{d\varphi} \simeq -\frac{\theta_E^2}{\varphi^2} = -\frac{1}{u^2}, \quad (44)$$

i.e. the change of the centroid shift with the distance falls off one power faster than the centroid shift itself, Eq. (9), however, 2 powers slower than the shift in magnitude, Eq. (7). With

$$\frac{d\varphi}{dt} = 58 \left(\frac{v}{100 \text{ km s}^{-1}} \right) \left(\frac{D_L}{1 \text{ kpc}} \right)^{-1} \mu\text{as days}^{-1}, \quad (45)$$

one gets

$$\begin{aligned} \frac{d\delta}{dt} &= \frac{d\delta}{d\varphi} \frac{d\varphi}{dt} \\ &= -58 \frac{\theta_E^2}{\varphi^2} \left(\frac{v}{100 \text{ km s}^{-1}} \right) \left(\frac{D_L}{1 \text{ kpc}} \right)^{-1} \mu\text{as days}^{-1}. \end{aligned} \quad (46)$$

For $D_S \gg D_L$, the angular Einstein radius θ_E is given by Eq. (40) and the time in which the angular separation between lens and source changes by θ_E is given by

$$\begin{aligned} t_E &= \theta_E / \mu \\ &= 35 \left(\frac{M}{0.5 M_\odot} \right)^{1/2} \left(\frac{D_L}{1 \text{ kpc}} \right)^{1/2} \times \\ &\quad \times \left(\frac{v}{100 \text{ km s}^{-1}} \right)^{-1} \text{ days}. \end{aligned} \quad (47)$$

This means that for a close encounter at a minimal angular separation of $\lesssim 1 \theta_E$, one has still a centroid shift of $\sim 2 \mu\text{as}$ at a time $t = 1000 t_E \sim 100 \text{ yr}$ after the closest encounter, a centroid shift of $\sim 20 \mu\text{as}$ at a time $t = 100 t_E \sim 10 \text{ yr}$, and a centroid shift of $\sim 200 \mu\text{as}$ at a time $t = 10 t_E \sim 1 \text{ yr}$, where the magnitude shift is only of the order of 10^{-4} .

⁶In fact, an even larger role is played by the sun and the solar planets, whose effect is being taken into account in the SIM mission (R. J. Allen 1998, private communication).

Since large contributions to the optical depth of astrometric microlensing are expected for small distances between lens and observer, the disk stars are expected to play the most important role regardless of where the source star is located.⁶

For sources in the Galactic bulge towards Baade's window ($l = -1^\circ$, $b = -4^\circ$), which is the field of interest for the photometric microlensing surveys towards the Galactic bulge, the mass density of the disk stars is approximately constant, so that the optical depth for centroid shifts larger than δ_T reads

$$\begin{aligned} \tau_{\delta,0} &= \frac{16\pi G^2}{c^4} D_S \frac{\overline{M} \rho_0}{\delta_T^2} \int_0^1 (1-x)^2 dx \\ &= \frac{16\pi G^2}{3 c^4} D_S \frac{\overline{M} \rho_0}{\delta_T^2} \\ &= 0.55 \left(\frac{D_S}{8.5 \text{ kpc}} \right) \left(\frac{\overline{M}}{0.5 M_\odot} \right) \times \\ &\quad \times \left(\frac{\rho_0}{0.08 M_\odot \text{ pc}^{-3}} \right) \left(\frac{\delta_T}{1 \mu\text{as}} \right)^{-2}. \end{aligned} \quad (48)$$

Values for $\tau_{\delta,0}$ for the reference values of \overline{M} and ρ_0 are shown in Table 1 for several values of δ_T . If one compares these values to the optical depth for light amplification

$$\tau_\mu(1) = 5.8 \cdot 10^{-7} \left(\frac{D_S}{8.5 \text{ kpc}} \right)^2 \left(\frac{\rho_0}{0.08 M_\odot \text{ pc}^{-3}} \right), \quad (49)$$

one sees that $\tau_\delta \gg 4\tau_\mu(1)$ and therefore the approximation $\tau_\delta(u_T^-, u_T^+) \approx \tau_\delta(0, \theta_E/\delta_T)$ is justified.

The case of an exponential behaviour of the mass density is discussed in Sect. 5.

4. ASTROMETRIC MICROLENSING EVENTS

4.1. The characteristics

Photometric microlensing is described by 3 characteristic quantities: The optical depth τ , the event rate Γ , and the average duration of an event $\langle t_e \rangle$, where one defines an event to last if the magnification exceeds a given threshold μ_T . These three characteristics are related by (Griest 1991)

$$\tau = \Gamma \langle t_e \rangle. \quad (50)$$

Consider coordinates in the lens plane, where the lens is at rest and the projected position of the source moves with a velocity $v = D_L \mu$. As discussed in Sect. 3, the magnification exceeds μ_T , if the position of the source projected onto the lens plane is in a circle of radius $u_T r_E$ around the lens. Optical depth, event rate, and average event duration can be related to the 'area', 'width', and 'average length' of this circle, respectively (Mao & Paczyński 1991; Dominik 1996). The area is given by $a = \pi u_T^2 r_E^2$. The width w is given by the range of impact parameters for which a moving source hits the area, in this case $w = 2 u_T r_E$. The average length \bar{l} is given by the average length of the portion of the source trajectory where the source is inside the area, in this case $\bar{l} = \frac{\pi}{2} u_T r_E$.

For the optical depth, the area of successful source positions is given by $\sigma_\tau = a = \pi u_T^2 r_E^2$. All sources within a rectangle with sides $w = 2 u_T r_E$ (perpendicular to the motion) and

TABLE 1
ASTROMETRIC MICROLENSING OPTICAL DEPTH

Detection threshold	Astrometric microlensing optical depth per observed star	
	Bulge stars towards Baade's window $\rho(x) = \rho_0$ $D_S = 8.5 \text{ kpc}$	Perpendicular to Galactic plane $\rho(x) = \rho_0 \exp\{-x D_S/H\}$ $D_S \gg H = 300 \text{ pc}$
$\delta_T (\mu\text{as})$	$\tau_{\delta,0}$	$\tau_{\delta,\infty}$
0.7	1.0	0.11
1	0.55	$5.8 \cdot 10^{-2}$
5	$2.2 \cdot 10^{-2}$	$2.3 \cdot 10^{-3}$
10	$5.5 \cdot 10^{-3}$	$5.8 \cdot 10^{-4}$
100	$5.5 \cdot 10^{-5}$	$5.8 \cdot 10^{-6}$

NOTE.—The astrometric microlensing optical depth $\tau_\delta \propto \rho_0 \overline{M} \delta_T^{-2}$ is shown as a function of the detection threshold δ_T for sources (i) towards the Galactic bulge and (ii) perpendicular to the Galactic plane, with the reference values $\overline{M} = 0.5 M_\odot$ and $\rho_0 = 0.08 M_\odot \text{ pc}^{-3}$, Eqs. (48) and (84).

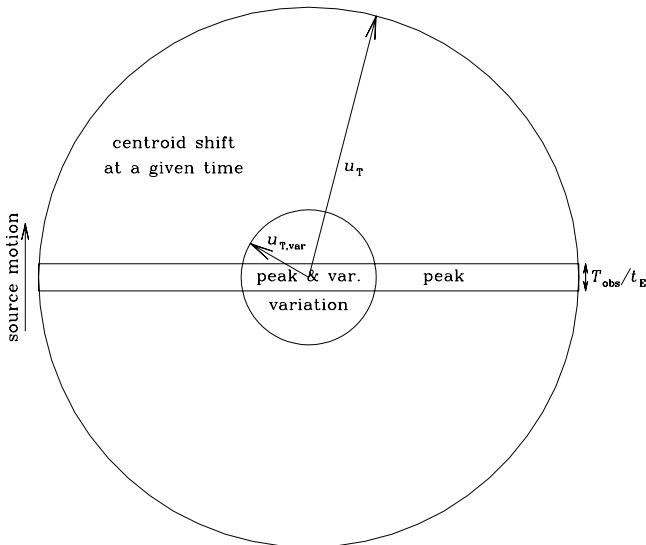


FIG. 4.— Regions σ in the lens plane that correspond to projected source positions that yield a given signature. All distances are given in multiples of the Einstein radius r_E . The lens is located in the center of the figure. The source moves in the indicated direction during the observation time T_{obs} , and the regions σ have been positioned with respect to the source position at the midpoint between the beginning and the end of the observations. The outer circle with radius $u_T = \theta_E/\delta_T$ includes the positions of the source where the centroid shift exceeds the threshold δ_T , the inner circle with radius $u_{T,\text{var}} = [(\theta_E T_{\text{obs}})/(\delta_T t_E)]^{1/2}$ includes the source positions for which the variation of the centroid shift during T_{obs} exceeds δ_T . Only for smaller regions, the closest approach between lens and source occurs within T_{obs} yielding a peak signature.

$T_{\text{obs}} v$ (parallel to the motion) will reach their closest approach to the lens within T_{obs} and thereby show a peak in their light curve. The area corresponding to events that peak within T_{obs} is therefore $\sigma_{\text{peak}} = 2 u_{\text{T}} r_{\text{E}} T_{\text{obs}} v$. Since every source that enters the area given by σ_{T} peaks exactly once, the event rate is given by $\Gamma = \gamma_{\text{peak}}/T_{\text{obs}}$. The average event duration is finally given by $\langle t_e \rangle = \bar{l}/v = \frac{\pi}{2} u_{\text{T}} t_{\text{E}}$.

For photometric microlensing, $u_{\text{T}} \sim 1$, and $\langle t_e \rangle \sim t_{\text{E}} \sim 1$ month, i.e. for $T_{\text{obs}} \sim 1$ yr, $\langle t_e \rangle \ll T_{\text{obs}}$. This means that one observes the events from baseline to peak and back to baseline. This implies that an event with a peak amplification of A_{peak} brightens by this amplification and fades back within T_{obs} , i.e. events that reach A_{T} also vary by A_{T} or more within the observation time.

Since $u_{\text{T}} \gg 1$ for typical astrometric events, the situation is quite different. Though in both cases, photometric and astrometric microlensing, only the variation of the signal (the magnification or the centroid shift) can be observed, not the signal itself, this difference strongly affects astrometric microlensing, while it does not affect photometric microlensing, unless t_{E} is very long. For astrometric microlensing, $\langle t_e \rangle \sim 200 t_{\text{E}} \sim 20$ yr, which may well exceed T_{obs} , so that one has to look for configurations where the signal *varies* by a given amount rather than for configurations where it exceeds some amount (compared to an asymptotic value which is unknown in this case).

As shown later, for small $\delta_{\text{T}} (\lesssim 10 \mu\text{as})$ and $T_{\text{obs}} \lesssim 10$ yr, the region of source positions for which the centroid shift varies by more than δ_{T} within T_{obs} can be approximately described by a circle of radius $u_{\text{T,var}} r_{\text{E}}$, where $u_{\text{T,var}} < u_{\text{T}}$, and $u_{\text{T,var}} \rightarrow u_{\text{T}}$ for $T_{\text{obs}} \rightarrow \infty$. Therefore, one has an analogous situation to the case where the criterion that the centroid shift exceeds δ_{T} is used: u_{T} just needs to be replaced by $u_{\text{T,var}}$. While the region $\sigma_{\text{var}} = \pi u_{\text{T,var}}^2 r_{\text{E}}^2$ corresponds to source positions giving rise to centroid shift variations larger than δ_{T} within T_{obs} , this does not give the event rate, because the same event may show a significant variation within subsequent time intervals. Instead, it is again useful to consider the closest approach between lens and source to occur within T_{obs} yielding a peak signature. The source positions yielding a significant variation and a peak signature are located within a rectangle with sides $u_{\text{T}} r_{\text{E}}$ (perpendicular to motion) and $T_{\text{obs}} v$ (parallel to motion), so that the area of successful source positions is $\gamma_{\text{var,peak}} = 2 u_{\text{T,var}} r_{\text{E}} T_{\text{obs}} v$. Figure 4 illustrates the regions yielding the different signatures.

While for $\langle t_e \rangle \ll T_{\text{obs}}$, the observed variation becomes identical with the maximum signal, for $\langle t_e \rangle \gtrsim T_{\text{obs}}$ it can happen that one sees a significant variation without reaching the peak and that one reaches the peak but does not see a significant variation. For the actual centroid shift being much larger than δ_{T} and the closest approach being reached within T_{obs} , the observed *variation* of the centroid shift during T_{obs} may fall below the threshold. On the other hand, the variation in the centroid shift can be larger than δ_{T} without reaching the maximal value within T_{obs} . In such a case, a monotonous variation of the centroid shift can be seen, which moreover points approximately into the same direction. The observed centroid of light also moves due to the proper motion of the source (and a luminous lens) and due to the parallactic motion and these motions have to be corrected for. In fact, for $u \gg 1$, the proper motion

can be many orders of magnitude larger than the centroid shift due to lensing. The centroid shift due to lensing can only be separated by detecting its different time behaviour. Therefore, the subset of events that also ‘peak’ within T_{obs} forms a class of events with a signature that is distinct from proper motion (and parallactic motion) and hence can be more easily detected and distinguished.

Note that the effective observation time can be substantially stretched just by making a few additional measurements after a few years.

4.2. Significant variation in an event

Let us investigate the change of centroid shift between two points of time separated by T_{obs} . Let p_0 denote the value of $p(t)$ (c.f. Eq. (13)) in the middle between these points and

$$\Delta p = \frac{T_{\text{obs}}}{2 t_{\text{E}}}. \quad (51)$$

For $u_0^2 + p_0^2 \gg 1$, the square of the absolute value of the change in centroid shift is given by

$$\begin{aligned} D^2(u_0, p_0 - \Delta p, p_0 + \Delta p) &= \\ &= \left| \vec{\delta}(u_0, p_0 + \Delta p) - \vec{\delta}(u_0, p_0 - \Delta p) \right|^2 \\ &= \left[\left(\frac{u_0}{u_0^2 + (p_0 + \Delta p)^2} - \frac{u_0}{u_0^2 + (p_0 - \Delta p)^2} \right)^2 + \right. \\ &\quad \left. + \left(\frac{p_0 + \Delta p}{u_0^2 + (p_0 + \Delta p)^2} - \frac{p_0 - \Delta p}{u_0^2 + (p_0 - \Delta p)^2} \right)^2 \right] \theta_{\text{E}}^2. \end{aligned} \quad (52)$$

For $(\Delta p)^2 \ll u_0^2 + p_0^2$ one obtains

$$D^2 = 4 \frac{(\Delta p)^2 \theta_{\text{E}}^2}{(u_0^2 + p_0^2)^2}. \quad (53)$$

In this limit, D is also the maximum change in the centroid shift within T_{obs} around p_0 ,⁷ so that the condition for a change in the centroid shift above the threshold means that (u_0, p_0) lie within a circle of radius

$$\begin{aligned} u_{\text{T,var}} &= \sqrt{\frac{2 \Delta p \theta_{\text{E}}}{\delta_{\text{T}}}} \\ &= \sqrt{\frac{T_{\text{obs}} \theta_{\text{E}}}{\delta_{\text{T}} t_{\text{E}}}} \\ &= \sqrt{\frac{T_{\text{obs}} v}{\delta_{\text{T}} D_{\text{L}}}}. \end{aligned} \quad (54)$$

Using reference values, $u_{\text{T,var}}$ reads

$$\begin{aligned} u_{\text{T,var}} &= 144 \left(\frac{\delta_{\text{T}}}{1 \mu\text{as}} \right)^{-1/2} \left(\frac{D_{\text{L}}}{1 \text{kpc}} \right)^{-1/2} \times \\ &\quad \times \left(\frac{v}{100 \text{km s}^{-1}} \right)^{1/2} \left(\frac{T_{\text{obs}}}{1 \text{yr}} \right)^{1/2}, \end{aligned} \quad (55)$$

⁷For $u_0 \gg 1$, the centroid-shift curve in space is a circle, so that the largest difference between two points within the traced time is the difference of the centroid-shift vectors at the boundary points if less than half the circumference is traced and the largest difference is equal to the diameter of the circle if half of the circumference or more is traced. For small Δp , one traces less than half the circumference. For $p^2 \geq u_0^2 + 2$, both components of $\vec{\delta}$ fall monotonously, so that the largest difference also occurs between the boundary points for small u_0 but larger $|p|$.

TABLE 2
PROBABILITY OF OBSERVING A SIGNIFICANT CENTROID-SHIFT VARIATION

Detection threshold	Probability of observing a centroid-shift variation larger than δ_T within $T_{\text{obs}} = 1$ yr for a given observed star	
	Bulge stars towards Baade's window $\rho(x) = \rho_0$ $D_S = 8.5$ kpc	Perpendicular to Galactic plane $\rho(x) = \rho_0 \exp\{-x D_S/H\}$ $D_S \gg H = 300$ pc
δ_T (μas)	$\gamma_{\text{var},0}$	$\gamma_{\text{var},\infty}$
1	$4.3 \cdot 10^{-3}$	$3.0 \cdot 10^{-4}$
5	$8.6 \cdot 10^{-4}$	$6.0 \cdot 10^{-5}$
10	$4.3 \cdot 10^{-4}$	$3.0 \cdot 10^{-5}$
100	$4.3 \cdot 10^{-5}$	$3.0 \cdot 10^{-6}$

NOTE.—The probability of observing a variation in the centroid shift larger than the threshold δ_T , $\gamma_{\text{var}} \propto \rho_0 T_{\text{obs}} v \delta_T^{-1}$, is shown for sources (i) towards the Galactic bulge, Eq. (65), and (ii) perpendicular to the Galactic plane, Eq. (90), with the reference values $T_{\text{obs}} = 1$ yr, $v = 100$ km s $^{-1}$, and $\rho_0 = 0.08 M_{\odot} \text{pc}^{-3}$.

which can be much smaller than u_T , though still $u_{T,\text{var}} \gg 1$. Let us now check the assumption $(\Delta p)^2 \ll u_{T,\text{var}}^2$, which becomes

$$\frac{T_{\text{obs}} \mu}{\theta_E} \ll 4 \frac{\theta_E}{\delta_T} \quad (56)$$

with Eq. (54), i.e. the change in the angular separation between lens and source in units of angular Einstein radii is much smaller than the ratio between (4 times) the angular Einstein radius and the centroid shift threshold δ_T . Eq. (56) can also be written as

$$F = \frac{\delta_T T_{\text{obs}} v}{4 \theta_E^2 D_L} \ll 1. \quad (57)$$

With $\langle t_e \rangle = \frac{\pi}{2} u_T t_E$, $u_T = \theta_E/\delta_T$, and $t_E = (D_L \theta_E)/v$, one sees that $F \ll 1$ reflects the condition $\langle t_e \rangle \gg T_{\text{obs}}$. For nearby lenses ($D_S \gg D_L$), one obtains

$$F = \frac{c^2 \delta_T T_{\text{obs}} v}{16GM} \quad (58)$$

$$= 1.3 \cdot 10^{-3} \left(\frac{M}{0.5 M_{\odot}} \right)^{-1} \left(\frac{T_{\text{obs}}}{1 \text{ yr}} \right) \times \left(\frac{v}{100 \text{ km s}^{-1}} \right) \left(\frac{\delta_T}{1 \mu\text{as}} \right), \quad (59)$$

so that the condition $F \ll 1$ is fulfilled for $\delta_T \lesssim 10 \mu\text{as}$ and $T_{\text{obs}} \lesssim 10$ yr.

The next-order corrections to the circle $u_0^2 + p_0^2 = u_{T,\text{var}}^2$ can be determined by looking at the cases $u_0 = 0$ and $p_0 = 0$. For $u_0 = 0$, one obtains from Eq. (52)

$$D^2 = \frac{4(\Delta p)^2}{[p_0^2 - (\Delta p)^2]^2} \theta_E^2, \quad (60)$$

so that the threshold δ_T is reached for ($p_0 > \Delta p$)

$$p_{0,T}^2 = \frac{T_{\text{obs}} v}{\delta_T D_L} \left(1 + \frac{T_{\text{obs}} v \delta_T}{4 \theta_E^2 D_L} \right) = \frac{T_{\text{obs}} v}{\delta_T D_L} (1 + F), \quad (61)$$

which reveals Eq. (54) for $F \ll 1$.

For $p_0 = 0$, one obtains

$$D^2 = \frac{4(\Delta p)^2}{[u_0^2 + (\Delta p)^2]^2} \theta_E^2, \quad (62)$$

so that the threshold δ_T is reached for

$$u_{0,T}^2 = \frac{T_{\text{obs}} v}{\delta_T D_L} \left(1 - \frac{T_{\text{obs}} v \delta_T}{4 \theta_E^2 D_L} \right) = \frac{T_{\text{obs}} v}{\delta_T D_L} (1 - F), \quad (63)$$

which reveals Eq. (54) for $F \ll 1$. This shows that F measures the asymmetry for $F \ll 1$.

Having found that a significant variation occurs for projected source positions within a circle of radius $u_{T,\text{var}} r_E$, if $F \ll 1$, the probability for having an event with a variation of the centroid shift of more than δ_T within a given time T_{obs} follows with $\sigma = \pi u_{T,\text{var}}^2 r_E^2$ from Eq. (27) as

$$\gamma_{\text{var}} = \frac{4\pi G}{c^2} D_S T_{\text{obs}} \frac{v}{\delta_T} \int_0^1 \rho(x) (1-x) dx. \quad (64)$$

Like the photometric optical depth τ_{μ} , γ_{var} does not depend on the lens masses.

For a constant mass density $\rho(x) = \rho_0$, one obtains

$$\begin{aligned} \gamma_{\text{var},0} &= \frac{2\pi G}{c^2} D_S T_{\text{obs}} \frac{v}{\delta_T} \rho_0 \\ &= 4.3 \cdot 10^{-3} \left(\frac{D_S}{8.5 \text{ kpc}} \right) \left(\frac{T_{\text{obs}}}{1 \text{ yr}} \right) \left(\frac{v}{100 \text{ km s}^{-1}} \right) \times \\ &\quad \times \left(\frac{\rho_0}{0.08 M_{\odot} \text{pc}^{-3}} \right) \left(\frac{\delta_T}{1 \mu\text{as}} \right)^{-1}. \end{aligned} \quad (65)$$

An exponential fall-off of the mass density is discussed in Sect. 5.

Values of γ_{var} as a function of the detection threshold δ_T for bulge sources towards Baade's window and perpendicular to the Galactic plane are given in Table 2.

4.3. Number of events

4.3.1. Significant centroid shift

Using the criterion $\delta > \delta_T$, one can calculate the event rate in analogy to the photometric case, and count the configurations where the a source reaches the closest approach to the lens within the observation time T_{obs} giving rise to a ‘peak’ signature. As pointed out before, the corresponding area is $\sigma_{\text{peak}} = 2 u_T r_E T_{\text{obs}} v$. If one compares this with the area corresponding to events that show significant variation $\sigma_{\text{var}} = \pi u_{T,\text{var}}^2 r_E^2$, one sees that $\sigma_{\text{peak}} = (2/\pi) \sigma_{\text{var}}$, since $u_{T,\text{var}}^2 = T_{\text{obs}} v / (\delta_T D_L)$ and $u_T = \theta_E / \delta_T = r_E / (\delta_T D_L)$. Using the results of the last sections, Eqs. (64) and (65), one obtains a constant event rate

$$\Gamma = \frac{8G}{c^2} D_S \frac{v}{\delta_T} \int_0^1 \rho(x) (1-x) dx, \quad (66)$$

and for $\rho(x) = \rho_0$,

$$\begin{aligned} \Gamma_0 &= \frac{4G}{c^2} D_S \frac{v}{\delta_T} \rho_0 \\ &= 2.7 \cdot 10^{-3} \left(\frac{D_S}{8.5 \text{ kpc}} \right) \left(\frac{v}{100 \text{ km s}^{-1}} \right) \times \\ &\quad \times \left(\frac{\rho_0}{0.08 M_\odot \text{ pc}^{-3}} \right) \left(\frac{\delta_T}{1 \mu\text{as}} \right)^{-1} \text{ yr}^{-1}. \end{aligned} \quad (67)$$

An exponential fall-off of the mass density is discussed in Sect. 5.

Values of Γ as a function of the detection threshold δ_T for bulge sources towards Baade’s window and perpendicular to the Galactic plane are given in Table 3.

4.3.2. Significant variation of centroid shift

As pointed out before, the actual value of the centroid shift is not measurable, only its temporal variation can be observed. Since it may take much longer than the observation time to reach a centroid shift smaller than the detection threshold, there is a difference between whether one considers $\delta > \delta_T$ or the variation of δ larger than δ_T . Let us consider the probability for a significant variation larger than δ_T and the closest approach between lens and source to happen within T_{obs} . Rather than $2 u_T r_E$, the characteristic width now becomes $2 u_{T,\text{var}} r_E$, and the area of source positions giving rise to a variation and a peak within T_{obs} is $\sigma_{\text{var,peak}} = 2 u_{T,\text{var}} r_E T_{\text{obs}} v = 2 T_{\text{obs}}^{3/2} v^{3/2} \delta_T^{-1/2} D_L^{-1/2} r_E$, so that with Eq. (27)

$$\begin{aligned} \gamma_{\text{var,peak}} &= 4 \sqrt{\frac{G}{c^2}} D_S \overline{M^{-1/2}} T_{\text{obs}}^{3/2} v^{3/2} \delta_T^{-1/2} \times \\ &\quad \times \int_0^1 \rho(x) \sqrt{1-x} dx, \end{aligned} \quad (68)$$

where

$$\overline{M^{-1/2}} = \int_0^\infty M^{-1/2} f_M(M) dM, \quad (69)$$

and for $\rho(x) = \rho_0$ one obtains

$$\gamma_{\text{var,peak},0} = \frac{8}{3} \sqrt{\frac{G}{c^2}} D_S \overline{M^{-1/2}} T_{\text{obs}}^{3/2} v^{3/2} \delta_T^{-1/2} \rho_0$$

$$\begin{aligned} &\approx 6 \cdot 10^{-4} \left(\frac{\overline{M^{-1/2}}}{(0.5 M_\odot)^{-1/2}} \right) \left(\frac{D_S}{8.5 \text{ kpc}} \right) \times \\ &\quad \times \left(\frac{T_{\text{obs}}}{1 \text{ yr}} \right)^{3/2} \left(\frac{v}{100 \text{ km s}^{-1}} \right)^{3/2} \times \\ &\quad \times \left(\frac{\rho_0}{0.08 M_\odot \text{ pc}^{-3}} \right) \left(\frac{\delta_T}{1 \mu\text{as}} \right)^{-1/2}. \end{aligned} \quad (70)$$

Note that no constant event rate $\Gamma_{\text{var}} = \gamma_{\text{var,peak}}/T_{\text{obs}}$ is yielded, instead $\Gamma_{\text{var}} \propto T_{\text{obs}}^{1/2}$. However, for $T_{\text{obs}} \rightarrow \infty$, $u_{T,\text{var}} \rightarrow u_T$, and Γ_{var} loses the T_{obs} -dependence.

The result for an exponential fall-off of the mass density is discussed in Sect. 5.

Values of $\gamma_{\text{var,peak}}$ as a function of the detection threshold δ_T for sources towards the Galactic bulge and perpendicular to the Galactic plane are given in Table 4.

5. MEASURING THE SCALE PARAMETERS OF THE GALACTIC DISK

Let us now leave the direction where the mass density is (approximately) constant and assume a general mass density profile of the form

$$\rho(R, z) = \rho_0 \exp \left\{ -\frac{R-R_0}{d} - \frac{|z|}{h} \right\}, \quad (71)$$

where R measures the radial position outwards from the Galactic center, z gives the coordinate perpendicular to the Galactic plane, R_0 is the radial position of the sun, ρ_0 is the local density of disk stars, d and h are scale lengths in the Galactic plane and perpendicular to it, where

$$\rho_0 \sim 0.08 M_\odot \text{ pc}^{-3}, \quad d \sim 3.5 \text{ kpc}, \quad h \sim 0.3 \text{ kpc}. \quad (72)$$

For a general direction characterized by the Galactic longitude and latitude (l, b) , one has

$$z = x D_S \sin b \quad (73)$$

and

$$R = R_0 \sqrt{1 + x^2 y^2 \cos^2 b - 2xy \cos b \cos l}, \quad (74)$$

where $y = D_S/R_0$. For $b = \pm\pi/2$ (towards the Galactic poles), one obtains $R = R_0$, so that

$$\rho(R, z) = \rho_0 \exp \left\{ -\frac{D_L}{h} \right\}, \quad (75)$$

while for $l = 0$ (towards any latitude towards the Galactic center), one obtains $R = R_0 |1 - xy \cos b|$, and especially for $b = l = 0$ (towards the Galactic center), $R = |R_0 - x D_S|$. For $l = 0$ and sources on the same side of the Galactic center as the sun, i.e. $D_L \cos b < R_0$, the mass density reads

$$\begin{aligned} \rho(R, z) &= \rho_0 \exp \left\{ -D_L \left(\frac{|\sin b|}{h} - \frac{\cos b}{d} \right) \right\} \\ &= \rho_0 \exp \left\{ -\frac{D_L}{H} \right\}, \end{aligned} \quad (76)$$

where

$$H = \left(\frac{|\sin b|}{h} - \frac{\cos b}{d} \right)^{-1}. \quad (77)$$

TABLE 3
RATE OF EVENTS WITH $\delta > \delta_T$

Detection threshold	Rate of events where the centroid shift exceeds the threshold δ_T per observed star	
	Bulge stars towards Baade's window $\rho(x) = \rho_0$ $D_S = 8.5 \text{ kpc}$	Perpendicular to Galactic plane $\rho(x) = \rho_0 \exp\{-x D_S/H\}$ $D_S \gg H = 300 \text{ pc}$
$\delta_T (\mu\text{as})$	$\Gamma_0 (\text{yr}^{-1})$	$\Gamma_\infty (\text{yr}^{-1})$
1	$2.7 \cdot 10^{-3}$	$1.9 \cdot 10^{-4}$
5	$5.4 \cdot 10^{-4}$	$3.8 \cdot 10^{-5}$
10	$2.7 \cdot 10^{-4}$	$1.9 \cdot 10^{-5}$
100	$2.7 \cdot 10^{-5}$	$1.9 \cdot 10^{-6}$

NOTE.—The rate of events $\Gamma = \gamma_{\text{peak}}/T_{\text{obs}} \propto \rho_0 v \delta_T^{-1}$ for which the centroid shift exceeds the threshold δ_T is shown for sources (i) towards the Galactic bulge, Eq. (67), and (ii) perpendicular to the Galactic plane, Eq. (90), with the reference values $v = 100 \text{ km s}^{-1}$, and $\rho_0 = 0.08 M_\odot \text{ pc}^{-3}$.

TABLE 4
PROBABILITY FOR SIGNIFICANT VARIATION AND PEAK

Detection threshold	Probability of observing significant variation and peak within $T_{\text{obs}} = 1 \text{ yr}$ for a given observed star	
	Bulge stars towards Baade's window $\rho(x) = \rho_0$ $D_S = 8.5 \text{ kpc}$	Perpendicular to Galactic plane $\rho(x) = \rho_0 \exp\{-x D_S/H\}$ $D_S \gg H = 300 \text{ pc}$
$\delta_T (\mu\text{as})$	$\gamma_{\text{var,peak},0}$	$\gamma_{\text{var,peak},\infty}$
1	$2.6 \cdot 10^{-4}$	$1.4 \cdot 10^{-5}$
5	$1.2 \cdot 10^{-4}$	$6.3 \cdot 10^{-6}$
10	$8.3 \cdot 10^{-5}$	$4.4 \cdot 10^{-6}$
100	$2.6 \cdot 10^{-5}$	$1.4 \cdot 10^{-6}$

NOTE.—The probability of observing a significant variation and a peak signature in an event $\gamma_{\text{var,peak}} \propto \rho_0 T_{\text{obs}}^{3/2} v^{3/2} \delta_T^{-1/2}$ during $T_{\text{obs}} = 1 \text{ yr}$ is shown for sources (i) towards the Galactic bulge, Eq. (70), and (ii) perpendicular to the Galactic plane, Eq. (92), with the reference values $v = 100 \text{ km s}^{-1}$, $M^{-1/2} = (0.5 M_\odot)^{-1/2}$, and $\rho_0 = 0.08 M_\odot \text{ pc}^{-3}$.

For $b_0^\pm = \pm \arctan(h/d) \sim \pm 4.9^\circ$, the mass density remains constant as $H \rightarrow \infty$, otherwise the mass density decreases exponentially for $|b| > |b_0|$ or increases exponentially for $|b| < |b_0|$ with D_L on the length scale H , which is equal to h for $b = \pm\pi/2$ and equal to d for $b = 0$ (increase) or $b = \pi$ (decrease), and a mixture of both scales in general.

With $s = D_S/H$, the exponential behavior given by Eq. (76) can be written in the form $\rho(x) = \rho_0 \exp\{-xs\}$, where $s > 0$ ($H > 0$) means an exponential decrease, $s < 0$ ($H < 0$) means an exponential increase, and $s = 0$ ($|H| \rightarrow \infty$) means a constant mass density.

The expectation value of the lens distance is yielded with Eqs. (35) and (37) as

$$\langle x \rangle = \frac{s^2 + 2s(e^{-s} - 2) + 6(e^{-s} - 1)}{s^3 - 2s^2 + 2s(1 - e^{-s})}. \quad (78)$$

For sources at distances $D_S \gg H$, one has $s \gg 1$, so that

$$\langle x \rangle = \frac{1}{s}, \quad (79)$$

which means that

$$\langle D_L \rangle = H, \quad (80)$$

i.e. the expectation value of the lens distance is equal to the scale parameter H of the exponential mass distribution.

For a constant mass density along the line-of-sight, the optical depth $\tau_{\delta,0}$ is proportional to the source distance D_S , so that the optical depth can be written as $\tau_{\delta,0} = \lambda_0 D_S$, where λ_0 does not depend on D_S . With Eq. (35), the optical depth for an exponential mass density reads

$$\tau_{\delta,s} = 3\tau_{\delta,0} \int_0^1 e^{-sx} (1-x)^2 dx. \quad (81)$$

The evaluation of the integral yields

$$\begin{aligned} \tau_{\delta,s} &= 3\tau_{\delta,0} \left[\frac{1}{s} - \frac{2}{s^2} + \frac{2}{s^3} (1 - e^{-s}) \right] \\ &= 3\lambda_0 H \left[1 - \frac{2}{s} + \frac{2}{s^2} (1 - e^{-s}) \right] \\ &= 3\lambda_0 H F(s). \end{aligned} \quad (82)$$

For $s \gg 1$, i.e. $D_S \gg H$, and exponential decrease, one obtains

$$F(s) \simeq 1 - \frac{2}{s}, \quad (83)$$

so that

$$\tau_{\delta,s} \simeq \tau_{\delta,\infty} = 3\lambda_0 H, \quad (84)$$

so that the optical depth measures the scale length H . This implies that for different directions, different combinations of the two disk scale parameters d and h are measured, which means that with the information from several directions, d and h can be determined. The case of constant mass density is revealed in the limit $s \rightarrow 0$, i.e. $H \rightarrow \infty$, where

$$\lim_{s \rightarrow 0} \frac{F(s)}{s} = \frac{1}{3}, \quad (85)$$

⁸Unfortunately, this view is obscured in the optical

⁹Consider e.g. the expansion of $\sqrt{1-x}$

so that $\tau_{\delta,s=0} = \tau_{\delta,0}$. For $s < 0$, the optical depth exceeds $\tau_{\delta,0}$. Using $D_S = R_0 = 8.5$ kpc and $d = 3.5$ kpc, one obtains for the optical depth towards the center of the Galaxy⁸

$$\tau_{\delta,-2.4}(H = d = 3.5 \text{ kpc}) = 2.6 \tau_{\delta,0}(D_S = 8.5 \text{ kpc}), \quad (86)$$

i.e. about 2.5 times larger than towards Baade's window.

For objects in the LMC ($D_S = 50$ kpc), one has approximately $(l, b) = (0, -\pi/2)$, so that one obtains for $h = 0.3$ kpc

$$\tau_{\delta,167}(H = h = 0.3 \text{ kpc}) = 0.10 \tau_{\delta,0}(D_S = 8.5 \text{ kpc}), \quad (87)$$

while for $h = 1$ kpc, one obtains

$$\tau_{\delta,50}(H = h = 1 \text{ kpc}) = 0.34 \tau_{\delta,0}(D_S = 8.5 \text{ kpc}). \quad (88)$$

Not only the optical depth turns out to be proportional to the scale parameter H for an exponential fall-off of the mass density and $D_S \gg H$, the probabilities for variations, peaks, and variation and peaks also share this property. Like the optical depth, for constant mass densities, the probabilities for significant variation $\gamma_{\text{var},0}$, for a peak $\gamma_{\text{peak},0}$, and for a significant variation and a peak $\gamma_{\text{var,peak},0}$ (Eqs. (65), (67), and (70)) are proportional to D_S , so that $\gamma_{\text{var},0} = \lambda_{\text{var},0} D_S$, $\gamma_{\text{peak},0} = \lambda_{\text{peak},0} D_S$, and $\gamma_{\text{var,peak},0} = \lambda_{\text{var,peak},0} D_S$, where $\lambda_{\text{var},0}$, $\lambda_{\text{peak},0}$, and $\lambda_{\text{var,peak},0}$ do not depend on D_S .

With Eq. (64), one obtains for the probability of significant variation for an exponential mass density

$$\begin{aligned} \gamma_{\text{var},s} &= 2 \gamma_{\text{var},0} \int_0^1 e^{-sx} (1-x) dx \\ &= 2 \gamma_{\text{var},0} \left[\frac{1}{s} + \frac{1}{s^2} (e^{-s} - 1) \right] \\ &= 2 \lambda_{\text{var},0} H \left[1 + \frac{1}{s} (e^{-s} - 1) \right], \end{aligned} \quad (89)$$

which yields for $s \gg 1$

$$\gamma_{\text{var},s} \simeq \gamma_{\text{var},\infty} = 2 \lambda_{\text{var},0} H, \quad (90)$$

A similar relation holds for γ_{peak} , since $\gamma_{\text{peak}} = (2/\pi) \gamma_{\text{var}}$.

The probability for events to show a peak and significant variation reads with Eq. (68)

$$\gamma_{\text{var,peak},s} = \frac{3}{2} \gamma_{\text{var,peak},0} \int_0^1 e^{-sx} \sqrt{1-x} dx. \quad (91)$$

For $s \gg 1$, the leading order of the integral yields $1/s$,⁹ so that

$$\gamma_{\text{var,peak},s} \simeq \gamma_{\text{var,peak},\infty} = \frac{3}{2} \lambda_{\text{var,peak},0} H. \quad (92)$$

TABLE 5
THE EFFECT OF UNRESOLVED LUMINOUS LENS STARS

Source magnitude	Correction factor for unresolved luminous lenses as a function of source magnitude	
	Bulge stars towards Baade's window $\rho(x) = \rho_0$ $D_S = 8.5 \text{ kpc}$	Perpendicular to Galactic plane $\rho(x) = \rho_0 \exp\{-x D_S/H\}$ $D_S \gg H = 300 \text{ pc}$
V_{source}	$\langle(1+g)^{-1}\rangle$	$\langle(1+g)^{-1}\rangle$
12	0.99	0.90
15	0.95	0.78
17	0.91	0.67
19	0.84	0.54

NOTE.—This table shows the effect of unresolved luminous lens stars on the number of astrometric microlensing events. The rate of events with centroid shift $\delta > \delta_T$ and the probability of observing a significant variation larger than δ_T within the observation time T_{obs} are decreased by a blending factor $1+g$. The table lists the expectation value $\langle(1+g)^{-1}\rangle$ for several source luminosities and a simple luminosity function as given by Bahcall & Soneira (1980). Note that there is no dependence on the mass function.

6. THE EFFECT OF A LUMINOUS LENS

For a luminous lens that is not resolved from the source where

$$g = \frac{L_L}{L_S} \quad (93)$$

is the ratio between the lens and the (unlensed) source apparent luminosities, one obtains for the magnification (c.f. Eq. (4))

$$\mu(u) = \frac{g}{1+g} + \frac{u^2 + 2}{(1+g)u\sqrt{u^2 + 4}}, \quad (94)$$

which gives for $u \gg 1$

$$\mu(u) = 1 + \frac{2}{(1+g)u^4}. \quad (95)$$

For the centroid shift relative to a source at rest (e.g. Boden et al. 1998) one obtains (c.f. Eq. (8))

$$\delta_S(u) = \frac{u(1 - gu\sqrt{u^2 + 4})}{u^2 + 2 + gu\sqrt{u^2 + 4}} \theta_E. \quad (96)$$

However, if one subtracts the proper motion of the apparent 'source' object, i.e. the centroid of light composed of source and luminous lens, one obtains the observed centroid shift due to lensing as

$$\delta(u) = \delta_S(u) + \frac{g}{1+g} u \theta_E \quad (97)$$

$$= \frac{u}{1+g} \frac{1+g(u^2 - u\sqrt{u^2 + 4} + 3)}{u^2 + 2 + gu\sqrt{u^2 + 4}} \theta_E, \quad (98)$$

which gives for $u \gg 1$

$$\delta(u) \simeq \frac{1}{(1+g)u} \theta_E, \quad (99)$$

i.e. the centroid shift is reduced by a factor $1+g$. Therefore the threshold for a centroid shift larger than δ_T becomes

$$u_T^{\text{blended}} = \frac{\theta_E}{(1+g)\delta_T}, \quad (100)$$

and the threshold for a variation larger than δ_T during the observing time T_{obs} becomes

$$u_{T,\text{var}}^{\text{blended}} = \sqrt{\frac{T_{\text{obs}} v}{(1+g)\delta_T D_L}}, \quad (101)$$

so that in the blended case the detection threshold δ_T is effectively increased by a factor $1+g$. Therefore, the optical depth τ_δ decreases by a factor $(1+g)^2$, the rate of events where the centroid shift exceeds the threshold and the probability of a significant variation within T_{obs} decrease by a factor $1+g$, while the probability of a significant variation and a peak signature within T_{obs} decreases by a factor $\sqrt{1+g}$.

Since the (disk) lens star is much closer than the source star, one might think that g is expected to be a large number. However, in a microlensing experiment, one will only pick the bright source stars, while the lens star is mostly a faint object. To obtain a more quantitative statement, let us assume a simple luminosity function for the lenses as given by Bahcall & Soneira (1980), Eq. (1), and calculate the expectation value $\langle(1+g)^{-1}\rangle$ that gives the correction factor for the rate of events where the centroid shift exceeds δ_T and for the probability that the centroid shift varies by more than δ_T within T_{obs} . The results are shown in Table 5. One sees that the effect is rather small for observing bulge stars towards Baade's window and somewhat larger for observing perpendicular to the Galactic plane. In the latter case, the values practically do not depend on D_S if $D_S \gg H$. For $V = 17$ sources, the suppression due to blending is $\sim 10\%$ towards Baade's window and $\sim 30\%$ perpendicular to the Galactic plane.

The luminosity function of Bahcall & Soneira (1980) does not take into account a dip around $M_V = 7$ and a peak around $M_V = 12$ (e.g. Kroupa, Tout, & Gilmore 1993), therefore overestimating the number of stars around $M_V = 7$ and underestimating the number of stars around $M_V = 12$. However, the

values given in Table 5 depend only weakly on the details of the luminosity function. The most important question about the luminosity function is up to what point at the low end it remains constant: Bahcall & Soneira (1980) took it to be constant up to $M_V = 19$ and being zero for $M_V < 19$. A luminosity function that is flat down to $M_V = 25$ would yield $\langle(1+g)^{-1}\rangle = 0.79$ (0.70) for a $V = 17$ ($V = 19$) source in a direction perpendicular to the Galactic plane, instead of $\langle(1+g)^{-1}\rangle = 0.67$ (0.54); the values for brighter sources are less strongly affected.

There is another effect: The formulae given above are valid only if the luminous lens is *not* resolved from the source star. If the angular resolution is θ_{res} , which is ~ 200 mas for GAIA and ~ 10 mas for SIM (see, e.g., Lindegren & Perryman 1996, for more details on GAIA, and Böker & Allen 1999, for more details on SIM), then this limit is reached for

$$\begin{aligned} u_{\text{res}} &= \frac{\theta_{\text{res}}}{\theta_E} \\ &= 100 \left(\frac{\theta_{\text{res}}}{200 \text{ mas}} \right) \left(\frac{M}{0.5 M_\odot} \right)^{-1/2} \times \\ &\quad \times \left(\frac{D_L}{1 \text{ kpc}} \right)^{1/2}, \end{aligned} \quad (102)$$

and lens and source are resolved for $u > u_{\text{res}}$. This means that the centroid-shift curves are those for a dark lens in the outer region $u > u_{\text{res}}$ and only influenced by a luminous lens in the inner region $u \leq u_{\text{res}}$ irrespective of how large the blend factor g is. By comparing u_{res} with the expressions for u_T , Eq. (41), and $u_{T,\text{var}}$, Eq. (55), one sees that u_{res} is typically smaller than u_T but can be larger or of the order of $u_{T,\text{var}}$. Therefore the calculated optical depth is not strongly affected by blending, despite the $(1+g)^2$ -dependence, because for most of the cases, the luminous lens is resolved from the source. For the other signatures, the effect of lens resolution plays a less important role, so that the corresponding probabilities are somewhat decreased due to the blending by the unresolved luminous lens. Should the angular resolution limit be significantly decreased to, say, ~ 10 mas for most of all discussed cases, the lenses would be resolved and therefore the event rates close to the dark lens case.

7. IMPLICATIONS FOR ASTROMETRIC SPACE MISSIONS

Upcoming space missions such as SIM and GAIA will provide astrometric measurements with an accuracy of ~ 4 – $60 \mu\text{as}$, thus enabling us to observe the centroid shifts caused by microlensing of stars.

SIM will provide measurements with an accuracy of about $4 \mu\text{as}$ on targets with $V < 20$ that it is pointed to. This will provide the possibility for high-accuracy astrometric follow-up observations of ongoing microlensing events. While there is a $\sim 2\%$ probability that disk stars lead to a centroid shift of the same order, the variation of this centroid shift during the event duration of the photometric microlensing event is much smaller, so that the astrometric signal due to the lens that has been responsible for the original microlensing alert is measured. If one continues to measure the astrometric signal on larger time scales $\gtrsim 10$ yr, one has to take into account a contamination due to astrometric microlensing by another lens in the galactic disk.

Contrary to SIM, GAIA will perform an 5-year-long all-sky survey primarily planned to measure parallaxes with high accuracy (Gilmore et al. 1998) but does not have the ability of point-

ing the instrument to a selected target. To observe the parallax ellipse, GAIA will perform several measurements on each target per year. For sources with $V < 10$, of which there are about 200,000 objects in the sky, the expected accuracy is $\sim 20 \mu\text{as}$; for sources with $V < 15$, of which there are about 25–35 million objects in the sky, the expected accuracy is $\sim 60 \mu\text{as}$; and for sources with $V < 20$, of which there are about 1 billion objects in the sky, the expected accuracy is ~ 1 mas.

Let us now use GAIA as an astrometric microlensing survey instrument and estimate the expected number of events. Concerning the direction of the observed stars, let us be conservative with regard to the number of astrometric microlensing events and consider a direction perpendicular to the Galactic plane, where the event rate is close to minimum. Let us first consider the bright ($V < 15$) stars. For an accuracy of $\delta_T = 60 \mu\text{as}$, one estimates with Eq. (41) $u_T \sim 30$. Therefore, one expects an average event duration (with Eqs. (47)) of $\langle t_e \rangle \sim 3$ – 4 yr. This is smaller than the time of the mission T_{obs} , so that events that reach a certain threshold also vary approximately by the same amount ($u_{T,\text{var}} \sim u_T$). We can therefore estimate the number of events simply from the event rate per observed star $\Gamma \sim 3 \cdot 10^{-6}/\text{yr}$ (Eqs. (67) and (90), Table 3). Multiplying this with the 25–35 million stars with $V < 15$, the 5 years of the mission and the blending factor of 0.78, one obtains about 400 events during the life-time of GAIA. For the fainter stars ($V < 20$), one obtains for $\delta_T = 1$ mas an event rate of $\sim 2 \cdot 10^{-7}/\text{yr}$, so that with 5 years time of the mission, 1 billion stars, and a blending factor of 0.47, one obtains about 500 events. The very bright stars ($V < 10$) are not expected to contribute significantly due to their small number. In total, this estimate gives about 1000 events from the GAIA mission. We have underestimated this number by the assumption that the mass falls off exponentially on a scale of 300 pc and by the assumption that all stars with $V < V_0$ are at $V = V_0$. On the other hand, we have overestimated that number by the assumption that a signal is detectable when it exceeds the noise threshold (i.e. signal-to-noise-ratio of 1). There is also a dependence on the sampling rate.

However, we expect the underestimations and the overestimations to cancel to a big part, so that our estimate indicates the right order. GAIA will thus observe a large sample of astrometric microlensing events which can be used to determine the mass and velocities of the lenses, and to determine the scale length and height of the Galactic disk.

8. SUMMARY AND OUTLOOK

Astrometric and photometric microlensing differ in two main points: First, the observed centroid shift is a function of both the dimensionless impact parameter u and the angular Einstein ring radius θ_E such that for a given u , the observed centroid shift is directly proportional to θ_E . On the other hand, the observed magnification is a dimensionless quantity which depends only on u and not on any other scale. Second, for large angular separations between the lens and the source, the centroid shift, being proportional to $1/u$, falls off much more slowly than the photometric magnitude shift which is proportional to $1/u^4$. Due to the dependence of the centroid shift on the angular Einstein radius, astrometric microlensing favors lenses close to the observer, while photometric microlensing favors lenses around half-way between observer and source. Therefore, one gets the largest centroid shifts from nearby objects, which are the Sun and the planets first, whose effect has to be corrected for, and then the disk stars. Because of the slower fall-off with the

dimensionless separation u in the astrometric case, detectable signatures occur for much larger angular separations, so that the average duration of an event $\langle t_e \rangle$ can become much larger than the observation time T_{obs} . For the effect of luminous lenses this means that one can expect the lens to be resolved from the source star in some of the cases that show observable signatures. We have shown that the probability that a disk star introduces a centroid shift larger than a given amount δ_T at a given time reaches unity for $\delta_T \sim 0.7 \mu\text{as}$ for sources towards the Galactic bulge at a latitude where the mass density of the disk stars is constant, which is a good approximation for Baade's window, while this probability is about 2% for $\delta_T = 5 \mu\text{as}$ (see Table 1). Though there is some chance that the centroid shift of a photometrically observed microlensing event, as observed e.g. by SIM, is disturbed by disk star lensing (a 2nd lens), this additional centroid shift is not expected to vary much during the observation time (\sim several months), so that the effect expected is a slightly shifted position and the variation of the centroid shift is determined only by the primary lens. Only if one extends the observations to ~ 10 yr after the peak, one has to take the contamination by disk stars into account.

It is also interesting to examine the expected results from a microlensing survey looking for centroid shifts rather than the magnification of stars. As stated earlier, the largest centroid shifts come from nearby objects, which gives an opportunity to infer information about the disk stars. For $\delta_T \lesssim 10 \mu\text{as}$ and $T_{\text{obs}} \lesssim 10$ yr, $\langle t_e \rangle \gg T_{\text{obs}}$. Since one can only measure the variation in the centroid shift, not its actual value, and since the astrometric signal does not drop to zero within T_{obs} , the condition that the centroid shift exceeds the threshold δ_T cannot be taken as criterion for an event. Instead, one has to rely strictly on the criterion that the centroid shift varies by more than the threshold δ_T . For $\langle t_e \rangle \ll T_{\text{obs}}$, as for most photometric microlensing events, these two criteria become equivalent. The probability that a source star in the Galactic bulge towards Baade's window shows a centroid shift variation larger than $5 \mu\text{as}$ within one year is $\sim 10^{-3}$, which is about 3 orders of magnitude larger than the probabilities for photometric

microlensing (see Table 2). Among the events that show significant variations, only a fraction (10 % for $\delta_T = 5 \mu\text{as}$) will have the closest angular separation between the lens and the source within the observing time, which will result in a clear 'peak' signature, namely an observed change of sign of the component of the centroid shift parallel to the relative proper motion between lens and source, and a maximum of the centroid-shift component transverse to it. Since every event 'peaks' once, the number of events that reach the peak within T_{obs} is related to the event rate, while events that show significant variations only can show this variation in subsequent time intervals.

For an exponential decrease of the mass density along the line of sight (as it would be the case for lines-of-sight at high Galactic latitudes), the probabilities for events are proportional to the scale parameter in that direction if the source stars are at a distance of a few times the scale parameter or more. For sources perpendicular to the Galactic plane, the probability for a variation by more than $5 \mu\text{as}$ and a peak within $T_{\text{obs}} = 1$ yr is $\sim 6 \cdot 10^{-6}$ (Table 4). By observing astrometric microlensing events in different directions, one can not only infer information about the total mass and the mass spectrum but also determine the scale length and scale height of the Galactic disk.

An advantage of astrometric over photometric observations is that the lens mass, distance, and velocity can be extracted individually from the observations (Høg et al. 1995; Miyamoto & Yoshii 1995; Walker 1995; Paczyński 1998; Boden et al. 1998).

We expect ~ 1000 astrometric microlensing events to be detected by the GAIA mission during its lifetime of 5 years.

Martin Dominik's work at STScI has been financed by research grant Do 629/1-1 from Deutsche Forschungsgemeinschaft, while his work in Groningen is financed by a Marie Curie Fellowship from the European Commission (ERBFM-BICT972457). It is a pleasure to thank Ron Allen, Torsten Böker, Stefano Casertano, Erik Høg, Mario Lattanzi, Michael Perryman, and Jayadev Rajagopal for helpful discussions regarding the details of the SIM and the GAIA missions.

REFERENCES

- Allen, R. J., Peterson, D., & Shao, M. 1997, in Proc. SPIE 2871, Optical Telescopes of Today and Tomorrow, ed. A. L. Ardeberg (Bellingham: SPIE), 504
- Bahcall, J. N., & Soneira, R. M. 1980, ApJS, 44, 73
- Boden, A. F., Shao, M., & Van Buren, D. 1998, ApJ, 502, 538
- Böker, T., & Allen, R.J. 1999, ApJ, in press (astro-ph/9903490)
- Dominik M. 1996, PhD thesis, Universität Dortmund
- Gilmore, G., Perryman, M., Lindegren, L., Favata, F., Høg, E., Lattanzi, M., Luri, X., Mignard, F., Roeser, S., & de Zeeuw, P. T. 1998, in Proc. SPIE 3350, Astronomical Interferometry, ed. R. D. Reasenberg (Bellingham: SPIE), 541
- Griest, K. 1991, ApJ, 366, 412
- Høg, E., Novikov, I. D., & Polnarev, A. G. 1995, A&A, 294, 287
- Kiraga, M., & Paczyński, B. 1994, ApJ, 430, 101
- Kroupa, P., Tout, C. A., & Gilmore, G. 1993, MNRAS, 262, 545
- Lindegren, L., & Perryman, M. A. C. 1996, A&AS, 116, 579
- Mao, S., & Paczyński, B. 1991, 374, L37
- Miralda-Escudé, J. 1996, ApJ, 470, L113
- Miyamoto, M., & Yoshii, Y. 1995, AJ, 110, 1427
- Paczynski, B. 1986, ApJ, 304, 1
- Paczynski, B. 1996, Acta Astron. 46, 291
- Paczynski, B. 1998, ApJ, 494, L23
- Sahu, K. C. 1994, Nature, 370, 265
- Walker, M. A. 1995, ApJ, 453, 37